

EXPERIMENTAL CONSTRAINTS ON THE CABIBBO-KOBAYASHI-MASKAWA MATRIX^a

S. MELE

CERN, CH1211, Genève 23, Switzerland

E-mail: Salvatore.Mele@cern.ch

The LEP investigation of the B_d^0 and B_s^0 oscillations and of the Cabibbo-Kobayashi-Maskawa matrix element $|V_{ub}|$ improve the constraints on the other elements of this matrix. From a fit to the experimental data and the theory calculations it is possible to determine the vertex of the unitarity triangle as:

$$\rho = 0.155_{-0.105}^{+0.115} \quad \eta = 0.383_{-0.060}^{+0.063}.$$

The corresponding values of its angles, in their customary definition in terms of sines for α and β , are:

$$\sin 2\alpha = 0.08_{-0.50}^{+0.43} \quad \sin 2\beta = 0.75 \pm 0.10 \quad \gamma = 68 \pm 15^\circ.$$

The fit also yields indirect information on the compatibility with zero of the CP violating phase of the matrix, on some non-perturbative QCD parameters and on the B_s^0 oscillation frequency.

1 Introduction

The Standard Model of the electroweak interactions¹ predicts a mixing of the quark mass and weak interaction eigenstates, as described by the Cabibbo-Kobayashi-Maskawa² (CKM) matrix. This 3×3 unitary matrix can be written³ in terms of only four real parameters:

$$\begin{pmatrix} V_{ud} & V_{us} & V_{ub} \\ V_{cd} & V_{cs} & V_{cb} \\ V_{td} & V_{ts} & V_{tb} \end{pmatrix} \simeq \begin{pmatrix} 1 - \frac{\lambda^2}{2} & \lambda & A\lambda^3(\rho - i\eta) \\ -\lambda & 1 - \frac{\lambda^2}{2} & A\lambda^2 \\ A\lambda^3(1 - \rho - i\eta) & -A\lambda^2 & 1 \end{pmatrix}. \quad (1)$$

A , ρ and η are of the order of the unity and λ is chosen as the sine of the Cabibbo angle. This parametrisation, that holds to order λ^4 , shows immediately the hierarchy of the couplings of the quarks in the charged current part of the Standard Model Lagrangian. Moreover, the parameter η gives the amount of the complex phase of the matrix and is thus directly related to the known violation of the CP symmetry produced by the weak interaction. The study of its compatibility with zero is thus of great interest.

The parameters A and λ are known with an accuracy of a few percent and the determination of ρ and η is presented in what follows. This can be achieved by means of a fit of the theory modelling of some physical processes to the experimental data.

^aTo appear in the Proceedings of the *Workshop on CP Violation*, Adelaide, July 3-8 1998.

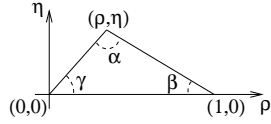


Figure 1: The unitarity triangle.

The measurement of the ρ and η parameters is usually associated to the determination of the only unknown vertex of a triangle in the ρ - η plane whose other two vertices are in $(0,0)$ and $(1,0)$. This triangle, called the unitarity triangle, is shown in Figure 1.

2 Constraints

The value of the sine of the Cabibbo angle is known with a good accuracy⁴ as:

$$\lambda = 0.2196 \pm 0.0023.$$

The parameter A depends on λ and on the CKM matrix element $|V_{cb}|$ and can be extracted as:

$$A = \frac{|V_{cb}|^2}{\lambda^2} = 0.819 \pm 0.035,$$

where it has been used⁴:

$$|V_{cb}| = (39.5 \pm 1.7) \times 10^{-3}.$$

The four physical processes that show the largest sensitivity to the values of the CKM parameters ρ and η are described below.

2.1 CP Violation for Neutral Kaons

The violation of the CP symmetry has been observed, to date, only in the neutral kaon system, whose mass eigenstates can be written as:

$$|K_S\rangle = p|K^0\rangle + q|\bar{K}^0\rangle \quad |K_L\rangle = p|K^0\rangle - q|\bar{K}^0\rangle.$$

The relation $p \neq q$ implies the violation of CP that, in the Wu-Yang phase convention⁵, is described by the parameter ϵ_K defined as:

$$\frac{p}{q} = \frac{1 + \epsilon_K}{1 - \epsilon_K}.$$

Information from the precise measurements of the $K_S \rightarrow \pi^+\pi^-$ and $K_L \rightarrow \pi^+\pi^-$ decay rates lead to the determination⁴:

$$|\epsilon_K| = (2.280 \pm 0.019) \times 10^{-3}.$$

The relation of $|\epsilon_K|$ with the CKM matrix parameters can be written^{6,7} as:

$$|\epsilon_K| = \frac{G_F^2 f_K^2 m_K m_W^2}{6\sqrt{2}\pi^2 \Delta m_K} B_K (A^2 \lambda^6 \eta) \times$$

$$\times [y_c (\eta_{ct} f_3(y_c, y_t) \eta_{cc}) + \eta_{tt} y_t f_2(y_t) A^2 \lambda^4 (1 - \rho)] \quad (2)$$

The functions f_3 and f_2 of the variables $y_i = m_i^2/m_W^2$ can be found in ⁸.

From the value of the mass of the top quark reported by the CDF and D0 collaborations ⁴, 173.8 ± 5.2 GeV, and the scaling proposed in ⁹ one obtains:

$$\overline{m}_t(m_t) = 166.8 \pm 5.3 \text{ GeV},$$

while the mass of the charm quark is ⁴:

$$\overline{m}_c(m_c) = 1.25 \pm 0.15 \text{ GeV}.$$

The QCD corrections are calculated ^{9,10,11} to be:

$$\eta_{cc} = 1.38 \pm 0.53, \quad \eta_{tt} = 0.574 \pm 0.004 \quad \text{and} \quad \eta_{ct} = 0.47 \pm 0.04.$$

The larger theoretical uncertainty that affects this constraint is that on the ‘‘bag’’ parameter B_K , that reflects non-perturbative QCD contributions to the process. Using the value of the JLQCD collaboration ¹², $B_K(2 \text{ GeV}) = 0.628 \pm 0.042$, with a calculation similar to that reported in ¹³, it is possible to derive:

$$B_K = 0.87 \pm 0.14.$$

The other physical constants of this and of the following constraints are reported in the left half of Table 1, whose numerical values not described in the text are all from ⁴. This constraint has the shape of an hyperbola in the $\rho - \eta$ plane.

2.2 Oscillations of B_d^0 Mesons

Neutral mesons containing a b quark show a behaviour similar to neutral kaons. The mass difference Δm_d of the two interaction eigenstates is the key feature of the physics while the lifetime difference dominates the effects in the neutral kaon system. The LEP experiments have measured Δm_d by investigating the oscillations of one CP eigenstate into the other ¹⁴:

$$\Delta m_d = 0.466 \pm 0.019 \text{ ps}^{-1}.$$

The relation of Δm_d with the CKM parameters, making use of the Standard Model description of the box diagrams that give rise to the mixing, is:

$$\Delta m_d = \frac{G_F^2}{6\pi^2} m_W^2 m_B^2 \left(f_{B_d} \sqrt{B_{B_d}} \right)^2 \eta_B y_t f_2(y_t) A \lambda^6 \left[(1 - \rho)^2 + \eta^2 \right]. \quad (3)$$

The calculated value of the QCD correction is ^{9,10,11}:

$$\eta_B = 0.55 \pm 0.01,$$

while the non-perturbative QCD parameter $f_{B_d}\sqrt{B_{B_d}}$, is taken as ¹⁵:

$$f_{B_d}\sqrt{B_{B_d}} = (0.201 \pm 0.042) \text{ GeV}.$$

This measurement of Δm_d constraints the vertex of the unitarity triangle to a circle in the $\rho - \eta$ plane, centred in $(1, 0)$.

2.3 Oscillations of B_s^0 Mesons

B_s^0 mesons are believed to undergo a mixing analogous to the B_d^0 ones, but their larger mass difference Δm_s is responsible for faster and thus still undetected oscillations. The combined LEP limit is ¹⁴:

$$\Delta m_s > 10.2 \text{ ps}^{-1} \text{ (95\% C.L.)}.$$

The expression for Δm_s in the Standard Model is similar to that for Δm_d and their ratio yields:

$$\Delta m_s = \Delta m_d \frac{1}{\lambda^2} \frac{m_{B_s}}{m_{B_d}} \xi^2 \frac{1}{(1 - \rho)^2 + \eta^2}. \quad (4)$$

All the theoretical uncertainties are included in the quantity ξ , evaluated as ¹⁵:

$$\xi = \frac{f_{B_d}\sqrt{B_{B_d}}}{f_{B_s}\sqrt{B_{B_s}}} = 1.14 \pm 0.08.$$

This experimental lower limit excludes all the values of the vertex of the unitarity triangle outside a circle in the $\rho - \eta$ plane with centre in $(1, 0)$.

2.4 Charmless Semileptonic b Decays

Each of the three constraints described above is affected by a large non-perturbative QCD uncertainty on some parameters, respectively B_K , $f_{B_d}\sqrt{B_{B_d}}$ and ξ . It follows from the CKM matrix parametrisation (1) that:

$$|V_{ub}|/|V_{cb}| = \lambda\sqrt{\rho^2 + \eta^2}. \quad (5)$$

An experimental determination of either $|V_{ub}|$ or the ratio $|V_{ub}|/|V_{cb}|$ is thus a constraint unaffected by these uncertainties.

The CLEO collaboration measured both the $|V_{ub}|/|V_{cb}|$ ratio and the value of $|V_{ub}|$ by means, respectively, of the endpoint of inclusive¹⁶ and exclusive¹⁷ charmless semileptonic b decays, obtaining the results:

$$|V_{ub}|/|V_{cb}| = 0.08 \pm 0.02 \quad \text{and} \quad |V_{ub}| = (3.3 \pm 0.2^{+0.3}_{-0.4} \pm 0.7) \times 10^{-3},$$

where the uncertainties on the second measurement are respectively statistical, systematic and theoretical. The ALEPH and L3 collaborations have recently measured at LEP the inclusive charmless semileptonic branching fraction of beauty hadrons, $\text{Br}(b \rightarrow X_u \ell \nu)$, from which the value of $|V_{ub}|$ can be extracted as in¹⁸. From the experimental results:

$$\begin{aligned} \text{ALEPH}^{19}: \quad \text{Br}(b \rightarrow X_u \ell \nu) &= (1.73 \pm 0.55 \pm 0.55) \times 10^{-3} \\ \text{L3}^{20}: \quad \text{Br}(b \rightarrow X_u \ell \nu) &= (3.3 \pm 1.0 \pm 1.7) \times 10^{-3}, \end{aligned}$$

where the first uncertainty is statistical and the second systematic, the following average can be obtained:

$$\text{Br}(b \rightarrow X_u \ell \nu) = (1.85 \pm 0.52 \pm 0.59) \times 10^{-3},$$

with the same meaning of the uncertainties. This value makes it possible to determine $|V_{ub}|$ at LEP by means of the formula described in¹⁸ as:

$$|V_{ub}| = (4.5^{+0.6}_{-0.7} {}^{+0.7}_{-0.8} \pm 0.2) \times 10^{-3}.$$

The first uncertainty is statistical, the second systematic and the third theoretical. The combination of this value with the CLEO exclusive one gives:

$$|V_{ub}| = (3.8 \pm 0.6) \times 10^{-3},$$

that, with the quoted value of $|V_{cb}|$, yields:

$$|V_{ub}|/|V_{cb}| = 0.093 \pm 0.016.$$

A circle in the $\rho - \eta$ plane with centre in $(0,0)$ represents this constraint. Figure 2a shows all the described constraints.

3 Fit Procedure and Results

The ρ and η parameters can be determined with the following fit procedure. The experimental and theoretical quantities that appear in the formulae describing the constraints have been fixed to their central values if their errors were below the 2%, and are reported in the left half of Table 1. The quantities affected by larger errors have been used as additional parameters of the fit,

including a constraint on their value. The following expression has then been minimised using the MINUIT package²¹:

$$\begin{aligned} \chi^2 = & \frac{(\widehat{A} - A)^2}{\sigma_A^2} + \frac{(\widehat{m}_c - m_c)^2}{\sigma_{m_c}^2} + \frac{(\widehat{m}_t - m_t)^2}{\sigma_{m_t}^2} + \frac{(\widehat{B}_K - B_K)^2}{\sigma_{B_K}^2} + \frac{(\widehat{\eta}_{cc} - \eta_{cc})^2}{\sigma_{\eta_{cc}}^2} + \\ & + \frac{(\widehat{\eta}_{ct} - \eta_{ct})^2}{\sigma_{\eta_{ct}}^2} + \frac{(f_{B_d} \widehat{\sqrt{B_{B_d}}} - f_{B_d} \sqrt{B_{B_d}})^2}{\sigma_{f_{B_d} \sqrt{B_{B_d}}}^2} + \frac{(\widehat{\xi} - \xi)^2}{\sigma_{\xi}^2} + \frac{\left(\frac{|\widehat{V}_{ub}|}{|\widehat{V}_{cb}|} - \frac{|V_{ub}|}{|V_{cb}|}\right)^2}{\sigma_{\frac{|V_{ub}|}{|V_{cb}|}}^2} + \\ & + \frac{(|\widehat{\epsilon}_K| - |\epsilon_K|)^2}{\sigma_{|\epsilon_K|}^2} + \frac{(\widehat{\Delta m}_d - \Delta m_d)^2}{\sigma_{\Delta m_d}^2} + \frac{(1 - \mathcal{A}(\Delta m_s))^2}{\sigma_{\mathcal{A}(\Delta m_s)}^2}. \end{aligned}$$

The symbols with a hat represent the reference values measured or calculated for a given physical quantity, as listed in the right half of Table 1, while the corresponding σ are their errors. The parameters of the fit are ρ , η , A , m_c , m_t , B_K , η_{cc} , η_{ct} , $f_{B_d} \sqrt{B_{B_d}}$ and ξ , that are used to calculate the values of $|\epsilon_K|$, Δm_d , Δm_s and $|V_{ub}|/|V_{cb}|$ by means of the formulae (2), (3), (4) and (5).

The Δm_s limit has been included in the χ^2 as suggested in²³. The results of the search for B_s^0 oscillations are combined¹⁴ in terms of the oscillation amplitude \mathcal{A} ²², a parameter that is zero if no oscillations are observed and is compatible with one in presence of a signal. The information on the dependence of both \mathcal{A} and its error on Δm_s is fully taken into account by comparing \mathcal{A} with one within its error.

The results of the fit are the following:

$$\rho = 0.155_{-0.105}^{+0.115} \quad \eta = 0.383_{-0.060}^{+0.063}.$$

The 95% Confidence Level regions for ρ and η are:

$$-0.10 < \rho < 0.35 \quad 0.27 < \eta < 0.50 \quad (95\% \text{C.L.}).$$

Figure 2b shows these confidence regions together with the favoured unitarity triangle, also superimposed on to the constraints of Figure 2a.

From these results it is also possible to determine the value of the angles of the unitarity triangle as:

$$\sin 2\alpha = 0.08_{-0.50}^{+0.43} \quad \sin 2\beta = 0.75 \pm 0.10 \quad \gamma = 68 \pm 15^\circ,$$

and, at the 95% of Confidence Level:

$$-0.75 < \sin 2\alpha < 0.94 \quad 0.54 < \sin 2\beta < 0.91 \quad 43^\circ < \gamma < 107^\circ \quad (95\% \text{C.L.}).$$

Table 1: Values of the physical constants (left) and parameters of the fit (right).

| | | | |
|--------------|--|--------------------------|-------------------------------|
| λ | $= 0.2196(23)$ | A | $= 0.819(35)$ |
| G_F | $= 1.16639(1) \times 10^{-5} \text{ GeV}^{-2}$ | η_{ct} | $= 0.47(4)$ |
| f_K | $= 0.1598(15) \text{ GeV}$ | η_{cc} | $= 1.38(53)$ |
| Δm_K | $= 0.5304(14) \times 10^{-2} \text{ ps}^{-1}$ | $\overline{m}_c(m_c)$ | $= 1.25(15) \text{ GeV}$ |
| m_K | $= 0.497672(31) \text{ GeV}$ | $\overline{m}_t(m_t)$ | $= 166.8(5.3) \text{ GeV}$ |
| m_W | $= 80.375(64) \text{ GeV}$ | $f_{B_d} \sqrt{B_{B_d}}$ | $= 0.201(42) \text{ GeV}$ |
| m_{B_d} | $= 5.2792(18) \text{ GeV}$ | B_K | $= 0.87(14)$ |
| m_{B_s} | $= 5.3962(20) \text{ GeV}$ | ξ | $= 1.14(8)$ |
| m_B | $= 5.290(2) \text{ GeV}$ | $ \epsilon_K $ | $= 2.280(19) \times 10^{-3}$ |
| η_B | $= 0.55(1)$ | Δm_d | $= 0.466(19) \text{ ps}^{-1}$ |
| η_{tt} | $= 0.574(4)$ | $ V_{ub} / V_{cb} $ | $= 0.093(16)$ |

The accuracy on $\sin 2\beta$ from these indirect studies is already of the same level of that expected to be achieved with the direct measurement at B-factories due to start in the near future.

4 Consequences of the Fit

As different models have been proposed to explain the CP violation in the neutral kaon system, it is of interest to remove from the fit the constraints related to this process and then investigate the compatibility of η with zero. This procedure yields the following results, also displayed in Figure 2c:

$$\rho = 0.126_{-0.084}^{+0.141} \quad \eta = 0.404_{-0.95}^{+0.70};$$

η is not compatible with zero at the 95% of Confidence Level either:

$$-0.120 < \rho < 0.366 \quad 0.176 < \eta < 0.540 \quad (95\% \text{C.L.}).$$

It is interesting to remove from the fit the constraints on the parameters affected by the largest theory uncertainty: B_K and $f_{B_d} \sqrt{B_{B_d}}$. This allows to extract information on their values and to determine ρ and η independently of these uncertainties. This method for the parameter B_K yields:

$$\rho = 0.126_{-0.084}^{+0.140} \quad \eta = 0.404_{-0.095}^{+0.069} \quad B_K = 0.76_{-0.16}^{+0.33}.$$

The favoured central value of B_K is lower than the input one, as suggested by other analyses¹⁰. The same procedure with $f_{B_d} \sqrt{B_{B_d}}$ as a free parameter

leads to the results:

$$\rho = 0.191_{-0.134}^{+0.121} \quad \eta = 0.378_{-0.060}^{+0.065} \quad f_{B_d} \sqrt{B_{B_d}} = 0.222_{-0.026}^{+0.030} \text{ GeV}.$$

The value of $f_{B_d} \sqrt{B_{B_d}}$ agrees with the predicted one and shows a smaller uncertainty.

The Δm_s constraint has a big impact on the ρ negative error as can be observed by removing it from the fit, what gives:

$$\rho = 0.155_{-0.204}^{+0.115} \quad \eta = 0.382_{-0.060}^{+0.064} \\ -0.46 < \rho < 0.35 \quad 0.27 < \eta < 0.51 \quad (95\% \text{C.L.}),$$

as shown in Figure 2d. The confidence regions for Δm_s can be extracted as:

$$\Delta m_s = 15.0_{-4.4}^{+4.7} \text{ ps}^{-1} \\ 5.6 \text{ ps}^{-1} < \Delta m_s < 23.9 \text{ ps}^{-1} \quad (95\% \text{C.L.}),$$

to be compared with the LEP expected sensitivity: $\Delta m_s < 13 \text{ ps}^{-1}$ ¹⁴.

5 Summary

The precise LEP measurements of Δm_d , the limits on Δm_s and the recent determination of $|V_{ub}|$ improve the constraints on the CKM matrix elements.

With a fit to these constraints it is possible to determine the vertex of the unitarity triangle:

$$\rho = 0.155_{-0.105}^{+0.115} \quad \eta = 0.383_{-0.060}^{+0.063},$$

what yields for its angles:

$$\sin 2\alpha = 0.08_{-0.50}^{+0.43} \quad \sin 2\beta = 0.75 \pm 0.10 \quad \gamma = 68 \pm 15^\circ.$$

The precision on $\sin 2\beta$ is comparable with the expected one from direct measurement at future B factories. Moreover, the presence of a complex phase in the matrix is established at more than the 95% of Confidence Level even removing from the analysis the constraints from the CP violation in the neutral kaon system. Assuming the Standard Model, the fit also gives:

$$f_{B_d} \sqrt{B_{B_d}} = 0.222_{-0.026}^{+0.030} \text{ GeV} \quad \Delta m_s = 15.0_{-4.4}^{+4.7} \text{ ps}^{-1}.$$

Acknowledgements

I am grateful to the organisers of this workshop for having invited me to present these results and to Joachim Mnich for the useful discussions on the fit procedure.

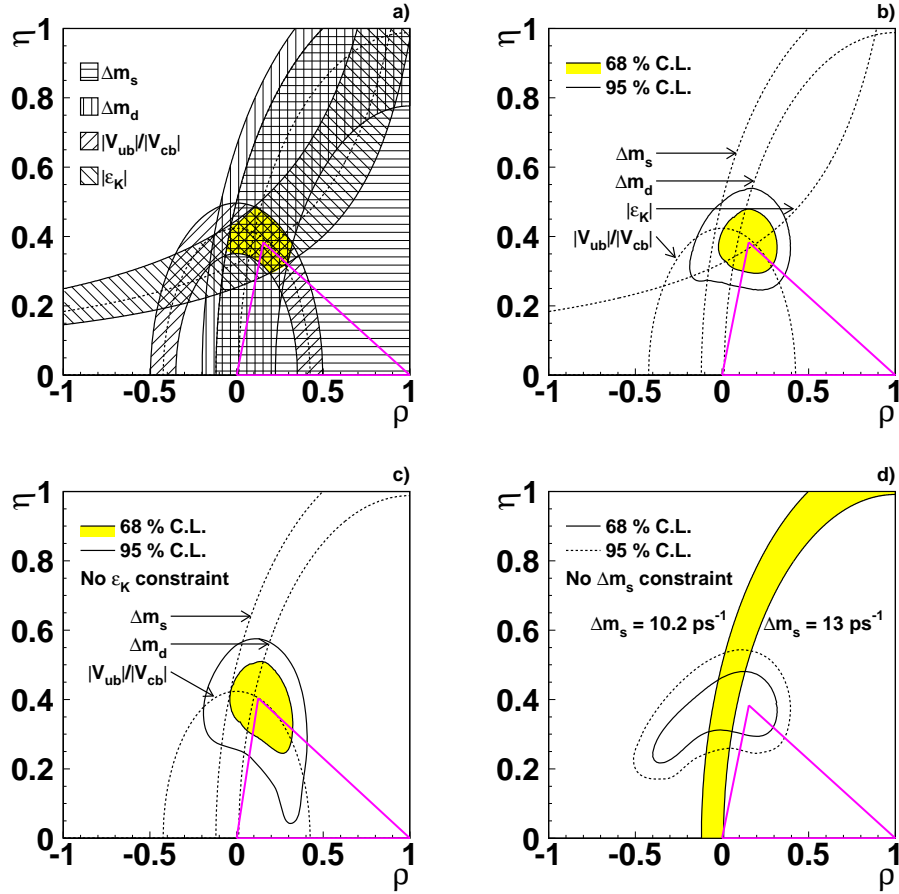


Figure 2: a) The constraints and the favoured unitarity triangle; the constraint coming from B_s^0 oscillations is a limit at 95% of Confidence Level, while the others represent a $\pm 1\sigma$ variation of the experimental and theoretical parameters entering the formulae in the text. b) c) and d) The fit unitarity triangle and the confidence regions for its vertex in the following assumptions: b) the fit to all the data, c) the constraints from the neutral kaon system are not applied, d) the constraint from the B_s^0 oscillations is not applied. The band in d) displays the values of ρ and η corresponding to a value of Δm_s between the lower limit and the LEP sensitivity. The central values of the constraints and the Δm_s limit are also shown in b) and c).

References

1. S. L. Glashow, *Nucl. Phys.* **22**, 579 (1961); S. Weinberg, *Phys. Rev. Lett.* **19**, 1264 (1967); A. Salam in Proceedings of the VIIIth Nobel Symposium, ed. by N. Svartholm (Almquist and Wiksell, Stockholm, 1968).
2. N. Cabibbo, *Phys. Rev. Lett.* **10**, 531 (1963); M. Kobayashi and K. Maskawa, *Prog. Theo. Phys.* **49**, 652 (1973).
3. L. Wolfenstein, *Phys. Rev. Lett.* **51**, 1945 (1983).
4. Particle Data Group, *Eur. Phys. J. C* **3**, 1 (1998).
5. T. T. Wu and C. N. Yang, *Phys. Rev. Lett.* **13**, 380 (1964).
6. A. J. Buras *et al.*, *Nucl. Phys. B* **238**, 529 (1984).
7. A. J. Buras *et al.*, *Nucl. Phys. B* **245**, 369 (1984).
8. A. Ali and D. London, *Z. Phys. C* **65**, 431 (1995).
9. A. J. Buras *et al.*, *Nucl. Phys. B* **347**, 491 (1990).
10. A. J. Buras, *Nucl. Instrum. Methods A* **368**, 1 (1995).
11. A. Buchalla *et al.*, *Nucl. Phys. B* **337**, 313 (1990); W. A. Kaufman *et al.*, *Mod. Phys. Lett. A* **3**, 1479 (1989); J. M. Flynn *et al.*, *Mod. Phys. Lett. A* **5**, 877 (1990); A. Datta *et al.*, *Z. Phys. C* **46**, 63 (1990); S. Herrlich *et al.*, *Nucl. Phys. B* **419**, 292 (1994).
12. JLQCD Collab., S. Aoki *et al.*, *Nucl. Phys. B(Proc. Suppl)* **63A-C**, 281 (1998).
13. S. R. Sharpe, *Nucl. Phys. B(Proc. Suppl)* **53**, 181 (1997).
14. R. Bately, XXXIIIrd Rencontres de Moriond, Electroweak Interactions and Unified Theories, 1998, to appear in the Proceedings.
15. J. M. Flynn and C. T. Sachrajda, preprint hep-lat/9710057 (1997), to appear in *Heavy Flavours* (2nd edition) ed. by A. J. Buras and M. Linder (World Scientific, Singapore).
16. CLEO Collab., J. Bartelt *et al.*, *Phys. Rev. Lett.* **71**, 4111 (1993).
17. CLEO Collab., A. Bean *et al.*, *Phys. Rev. Lett.* **70**, 2861 (1993); CLEO Collab., J. P. Alexander *et al.*, *Phys. Rev. Lett.* **77**, 5000 (1996).
18. N. G. Uraltsev, *Int. Jour. of Mod. Phys. A* **11**, 515 (1996); I. Bigi *et al.*, *Ann. Rev. Nucl. Part. Sci.* **47**, 591 (1997).
19. ALEPH Collab., R. Barate *et al.*, Preprint CERN-EP/98-067 (1998).
20. L3 Collab., M. Acciarri *et al.*, Preprint CERN-EP/98-097 (1998).
21. F. James, MINUIT Reference Manual, CERN Program Library Long Writeup D506, (1994).
22. H. G. Moser and A. Roussarie, *Nucl. Instrum. Methods A* **384**, 491 (1997).
23. F. Paganini *et al.*, Preprint LAL-97-79 (1997).